

NOTICE: This is the author's version of a work that was accepted for publication in Journal of Materials Science and Technology. Changes resulting from the publishing process, such as peer review, editing, corrections, structural formatting, and other quality control mechanisms may not be reflected in this document. Changes may have been made to this work since it was submitted for publication. A definitive version was subsequently published in Journal of Materials Science and Technology, Volume 29, Issue 11, November 2013, Pages 1059-1066. <http://dx.doi.org/10.1016/j.jmst.2013.08.001>

Accepted Manuscript

Prediction of Failure Modes during Deep Drawing of Metal Sheets with Nickel Coating

Jie Wu, Zengsheng Ma, Yichun Zhou, Chunsheng Lu



PII: S1005-0302(13)00173-4

DOI: [10.1016/j.jmst.2013.08.001](https://doi.org/10.1016/j.jmst.2013.08.001)

Reference: JMST 172

To appear in: *Journal of Materials Science & Technology*

Received Date: 16 May 2012

Revised Date: 16 January 2013

Please cite this article as: J. Wu, Z. Ma, Y. Zhou, C. Lu, Prediction of Failure Modes during Deep Drawing of Metal Sheets with Nickel Coating, *Journal of Materials Science & Technology* (2013), doi: 10.1016/j.jmst.2013.08.001.

This is a PDF file of an unedited manuscript that has been accepted for publication. As a service to our customers we are providing this early version of the manuscript. The manuscript will undergo copyediting, typesetting, and review of the resulting proof before it is published in its final form. Please note that during the production process errors may be discovered which could affect the content, and all legal disclaimers that apply to the journal pertain.

Prediction of Failure Modes during Deep Drawing of Metal Sheets with Nickel Coating

Jie Wu^{1,2)}, Zengsheng Ma^{1,2)*}, Yichun Zhou^{1,2)†}, Chunsheng Lu³⁾

- 1) Key Laboratory of Low Dimensional Materials and Application Technology of Ministry of Education, Xiangtan University, Xiangtan 411105, China
- 2) Faculty of Materials, Optoelectronics and Physics, Xiangtan University, Xiangtan 411105, China
- 3) Department of Mechanical Engineering, Curtin University, Western Australia 6845, Australia

[Manuscript received 16 May 2012, in revised form 16 January 2013]

*Corresponding author. Ph.D.; Tel.: +86 731 58293586; Fax: +86 731 58293468; E-mail address: zsma@xtu.edu.cn (Z. Ma);

†Corresponding author. Prof.; Tel.: +86 731 58293586; Fax: +86 731 58293468; E-mail address: zhouyc@xtu.edu.cn (Y. Zhou).

Corresponding author for Elsevier: Dr. Zengsheng Ma, zsma@xtu.edu.cn

To optimize the process parameters, it is necessary to exactly predict failure modes during deep drawing of coated metal sheets, where two main failure forms are fracture and wrinkling. In this paper, finite element simulations based on continuous damage mechanics were used to study the failure behavior during a cylindrical deep drawing of metal sheets with nickel coating. It is shown that taking the effect of blank holder force into account, these two failure modes can be predicted. The simulation results are well consistent with that obtained from experiments.

KEY WORDS: Failure; Deep drawing; Coated metal sheet; Damage

1. Introduction

Deep drawing is one of the most popular processes for transforming flat metallic sheet blanks into cup or box shaped parts in automotive and aerospace industries. During the process of deep drawing, metallic sheets are subjected to the large irreversible deformation, and two primary failure modes of fracture and wrinkling may appear^[1]. Huge design and control efforts have been made to eliminate the occurrence of failure through the proper design of blank^[2], tooling configuration^[3], and the selection of process parameters^[4]. Using the traditional trial-and-error approach, one-fourth or more time spends on the design and control procedure^[5]. Fortunately, with development of finite element methods and computer technologies, numerical

simulations can be used to model the forming process. In addition to avoiding long and expensive trial and error procedures, a better understanding on the metal forming process can also be obtained.

In finite element simulations, a forming limit diagram (FLD) is widely applied to analyze the fracture phenomena following the pioneering work of Keeler^[6] and Goodwin and Cuczynski^[7]. Based on major and minor strains, FLD is associated with the strain path; hence, a forming limit stress diagram was suggested^[8]. Signorelli et al.^[9] obtained FLD considering the influence of strain rate using a rate-dependent polycrystal self-consistent plasticity model. Hu et al.^[10] proposed a new FLD by introducing the effect of temperature and strain rate. The FLD provides the foundation of research on the fracture behavior during deep drawing of metal sheets. By comparing the strain status corresponding to elements, one can estimate whether or not fracture behaviors appear during forming^[11]. However, FLD does not have a predictive nature^[12]. In particular, it is impossible to predict when and where a failure can appear, and which failure mode may occur in work piece during a forming operation.

There have been many works on the prediction of fracture in the single layer sheet metal forming by finite element modeling based on ductile damage. Saanouni^[13] predicted the fracture area in hydro-bulging tests with an ellipsoidal matrix by ductile damage evolution. Based on Saanouni's theory, Khelifa and Oudjene^[12] investigated deep drawing (i.e., Swift's test) of aluminum sheets. Fan^[14] studied the crack initiation during deep drawing of square cups with different frames of ductile damage evolution. However, there have been few studies on the prediction of the failure behavior during deep drawing of a coated metal sheet.

Recently, more and more coated and pre-coated metal sheets have been used due to their good wear or corrosion resistance and decorative performance^[15]. There are different types of coating and substrate systems, such as hot-dip galvanized/steel or electro-galvanized/steel sheets^[16], nickel coating/steel^[17,18] or zinc phosphate coatings/steel sheets^[19], brass/steel two layer sheets^[20], and Fe/Al laminated composite sheets^[21]. The metal sheet with nickel coating (MSNC) is a typical type of material for safeguard in engineering. This material possesses good corrosion resistance, attractive toughness, and excellent plasticity, which offer potential for advanced structural engineering applications. In addition, the good adhesion between electrodeposited nickel coating and substrate is another advantage in practical applications^[22]. During the forming of a coated metal sheet, there is a failure mode like wrinkling^[23] or fracture^[21] appearing in a single layer sheet, as shown in **Fig. 1**. Thus, it is important to clarify

which failure mode occurs for a set of given parameters.

In this work, finite element models based on continuous damage mechanics were used to predict failure behaviors during a cylindrical deep drawing of MSNC. Two main failure modes (fracture and wrinkling) were studied under the condition of the blank holder force. A set of experiments were performed to verify simulation results and their abilities to predict the failure behavior in a work-piece during deep drawing.

2. Finite Element Simulations

2.1. Continuous damage mechanics

In the finite element package ABAQUS, there is a general framework for modeling damage and failure. Material failure is related to the complete loss of load-carrying capacity and thus results in the progressive degradation of stiffness. Continuous damage is a phenomenological model for predicting the onset of damage due to nucleation, growth, and coalescence of voids. Many researchers have used the continuous damage mechanics and the triaxiality dependent failure criteria to predict fracture in sheet metal forming^[24–26]. For example, Li et al.^[26] reported an extensive numerical and experimental study of the deep-drawing process leading to initiation and propagation of cracks based on the continuous damage mechanics.

The model assumes that the equivalent plastic strain $\bar{\varepsilon}_D^{pl}$ at the onset of damage is a function of stress triaxiality and strain rate, that is

$$\bar{\varepsilon}_D^{pl} = f(\eta, \dot{\varepsilon}^{pl}) = \frac{\varepsilon_T^+ \sinh[k_0(\eta^- - \eta)] + \varepsilon_T^- \sinh[k_0(\eta - \eta^+)]}{\sinh[k_0(\eta^- - \eta^+)]} \quad (1)$$

where $\eta = \sigma_m / \bar{\sigma}$ is the stress triaxiality with $\eta^+ = 2/3$ and $\eta^- = -2/3$ for isotropic materials in equibiaxial tensile and compressive deformation states, with $\sigma_m = (\sigma_1 + \sigma_2 + \sigma_3)/3$ and the von

Mises equivalent stress $\bar{\sigma} = \left[\frac{1}{2}(\sigma_1 - \sigma_2)^2 + (\sigma_2 - \sigma_3)^2 + (\sigma_3 - \sigma_1)^2 \right]^{1/2}$, $\dot{\varepsilon}^{pl} = \sqrt{2/3} \dot{\varepsilon}_{ij}$ is the

equivalent plastic strain rate, ε_T^+ and ε_T^- correspond to equivalent plastic strains at ductile damage initiation for equibiaxial tensile and compressive deformation, respectively, and k_0 is

a material parameter related to anisotropy. For isotropic materials, k_0 is equal to 1. The criterion for damage initiation is met when the following condition is satisfied

$$w_D = \int \frac{d\bar{\epsilon}^{pl}}{\bar{\epsilon}_D^{pl}(\eta, \dot{\bar{\epsilon}}^{pl})} = 1 \quad (2)$$

where w_D is a state variable that increases monotonically with plastic deformation. At each increment, the incremental increase of w_D is calculated by

$$\Delta w_D = \frac{\Delta \bar{\epsilon}^{pl}}{\bar{\epsilon}_D^{pl}(\eta, \dot{\bar{\epsilon}}^{pl})} \geq 0 \quad (3)$$

The geometrical method is adopted in our simulation as the wrinkling criterion, which directly measures wrinkle dimensions of deformed mesh. The wrinkle amplitude was measured from the gap between blank holder surface and die surface. The critical wrinkle amplitudes for determining the existence of a flange wrinkle is chosen to be at 8% nominal sheet thickness^[27].

2.2. Finite element model

The dynamic explicit code ABAQUS/Explicit is used to simulate the cylindrical deep drawing of MSNC. The tool and coated metal sheet in a deep drawing process is illustrated in Fig. 2(a). The forming tools such as die, punch and blank holder are considered as rigid bodies and their length parameters are shown in Fig. 2(b). The gap between die and blank holder for safe products is equal to 0.5 mm, as shown in Fig. 2(a). Because of symmetry of the sample, only a quarter of blank is chosen in modeling, as shown in Fig. 3(a). The original point of the coordinate system is located at the center of blank with thickness being the y direction. The die is fixed in the process of deep drawing and punch can move in the y direction. For the blank sheet, boundary conditions can be described as

$$u_z = 0, \quad M_x = 0, \quad M_y = 0 \quad \text{on the surface of } z = 0,$$

$$u_x = 0, \quad M_y = 0 \quad \text{and} \quad M_z = 0 \quad \text{on the surface of } x = 0,$$

$$u_z = 0, \quad M_x = 0 \quad \text{and} \quad M_z = 0 \quad \text{at the original point } u_x = 0.$$

The blank is a low carbon steel sheet of 0.3 mm thickness with double-side electrodeposited 3 μm thickness nickel coating. Both coating and substrate are modeled as an isotropic elastic–plastic material with exponential hardening. The true stress–strain relationship is given by

$$\varepsilon = \begin{cases} \sigma / E & \sigma \leq \sigma_y \\ (\sigma_y / E)(\sigma / \sigma_y)^{1/n} & \sigma \geq \sigma_y \end{cases} \quad (4)$$

where σ_y is the initial yield stress, n is the strain hardening exponent, E and ν are Young's modulus and Poisson's ratio, respectively. Material properties of nickel coating and low carbon steel substrate used in simulations are listed in Table 1^[28]. In our simulations, it is shown that the deviation is very small (~1%) between two results obtained by using the number of eight-node, linear brick, reduced integration (C3D8r) elements of 31518 and ~50000, respectively. Thus, the former is used in simulations of Ni coating metal sheets, as shown in Fig. 3(b) and (c). The interface between coating and substrate is assumed to be perfect because of the strong adhesion between nickel coating and substrate^[22].

During deep drawing of MSNC, the blank holder force (BHF) is one of the most important parameters. For a small BHF, wrinkles may appear in flange of drawn parts. When increasing the BHF, normal stress in the thickness direction increases, which restrains formation of wrinkles, and thus fracture may occur at the cup wall and punch profile. Three constants of BHF (2 kN, 1.5 kN, 1 kN) are applied in a deep drawing process.

3. Experimental

To verify the results of finite element simulations, deep drawing experiments of cylindrical flat punches were performed on a RG2000 micromachine-controlled universal tensile machine with the tool geometry shown in Fig. 2. Experiments were carried out by using oil based lubricant to punch, blank holder, and die surfaces as well as to both surfaces of blank. The friction coefficient between tools and blank is the same as that in simulations, ~0.1^[29]. All the three BHF are also the same as that used in finite element modeling.

4. Results and Discussion

4.1. Distribution of field variables

In the case of wrinkling, the distribution of damage at different punch displacements u in nickel coating is shown in Fig. 4(a). It is seen that damage increases with the increase of punch displacements. This is also seen from the damage contours at different punch displacements of 4, 6, 8 and 10 mm, as shown in Fig. 4(b). Accordingly, stress contours in the thickness

direction, σ_{22} and true strain distributions in the thickness direction, ϵ_{22} are shown in Fig. 4(c) and (d), respectively. When the punch displacement increases, the values of stress and strain increase. There are the same behaviors in the cases of success and fracture, as shown in Figs. 5 and 6. Damage arrives to 1 in fracture and wrinkling, which refers to the occurrence of failure. In Figs. 5 and 6, the damage and stress distributions in the thickness direction, σ_{22} and true strain distributions in the thickness direction, ϵ_{22} are shown in success and fracture at different punch displacements of 4, 6, 8 and 10 mm. Fig. 7 exhibits damage as a function of punch displacement u . Wrinkling takes place in the flange area, where damage firstly arrives at 1 when the punch displacement is 10 mm. Damage is less than 1 in the flange area in fracture and success. Fracture occurs at the punch fillet radius of a cup, where damage is equal to 1.

In the flange area, the maximum principal strain in wrinkling is much larger than that in fracture and success, as shown in Fig. 8. While the maximum principal strain in fracture is much larger than that in wrinkling and success at the punch fillet radius, as shown in Fig. 9(a) and (b).

4.2. Failure modes

In consideration of the influence of a blank holder force, two main failure modes (fracture and wrinkling) were predicted in simulations. The failure modes are judged from the distribution of displacements of blank in the thickness direction along a path from center to edge. As shown in Fig. 10(a), fracture occurs when the punch displacement is equal to 8 mm, where the displacement of blank in the thickness direction is discontinuous in wall areas. The fracture area is located at the punch fillet radius. In the case of success shown in Fig. 10(b), the displacement of blank in the thickness direction is continuous in wall areas. In wrinkling, the displacement of blank in the thickness direction in flange areas is much larger than that in fracture and success, as shown in Fig. 10(b) and (c).

The failure modes are judged by using punch load–displacement curves. Fig. 11 shows a comparison of punch load–displacement curves obtained by finite element simulations and experiments in the wrinkling mode. The punch load firstly increases to 9.1 kN with the punch displacement, and then decreases to 5 kN at the displacement of 13.6 mm, as shown in Fig. 11. It is found that some parts of MSNC have been drawn into the die cavity. The actual BHF exerted on blank decreases. The normal stress in the thickness direction of blank cannot

suppress the excessive metal flow. As predicted, wrinkling occurs in the flange of MSNC. Then, the punch load increases to another value of 9.2 kN at the displacement of 16.6 mm. This is because wrinkling makes blank with nickel coating draw into the die cavity more difficultly. Finally, the flange area is totally drawn into the die cavity, leading to decrease of the punch load.

As shown in Fig. 12, the comparison of deformation shapes between experiments and finite element simulations is based on continuous damage mechanics. When BHF is high, the normal stress in the thickness direction of blank suppresses the formation of wrinkles. But high BHF leads to insufficient metal flow and thus fracture occurs in a deep drawing process. The sharply decreasing punch load indicates the fracture of MSNC, which is located at the circumference zone contacting the punch radius. The punch displacement is equal to 7 mm when fracture occurs, which agrees with the experimental value of 6.8 mm. Similarly, as shown in Fig. 13, the punch load firstly increases to a maximum value of 10 kN when the punch displacement is 8.7 mm, and then decreases with increasing the punch displacement. When the punch displacement reaches about 23 mm, MSNC is totally drawn into the die cavity.

4.3. Comparison of strain status

In a deep drawing procedure, the risk of fracture and wrinkling can be evaluated by using the forming limit curve defined in the plane of principal strains^[30]. The strain status in fracture, wrinkling and success during finite element simulations is shown in Fig. 14, which is along a path from the center to edge of blank. The forming limit curve is extracted from our early studies^[17,31]. The points located above the forming limit curve represent fracture of blank with nickel coating. In the case of success, all the points locate in the safe area, and in wrinkling, a lot of points locate in areas where the minor strain is larger than the major strain. This area shows a tendency to wrinkling or fully developed wrinkles.

5. Conclusion

In this paper, the failure modes of nickel coating during deep drawing have been successfully predicted by using finite element simulations. A set of experiments were performed to test and verify the accuracy of finite element modeling. According to simulations, failure modes are affected by the blank holder force. For the relative low BHF, wrinkling takes place in the flange of nickel coating sheet, and for the relative high BHF, fracture occurs along a circumference zone in contact with the punch radius. The accuracy of finite element modeling

has been confirmed by experiments. The results show that finite element simulations based on continuous damage mechanics are a promising method in predicting failure modes during deep drawing of coated metal sheets.

Acknowledgements

This work was supported by the National Natural Science Foundation of China (Nos. 51172192 and 11102176), Hunan Provincial Natural Science Foundation of China (No. 09JJ3003), the Natural Science Foundation of Hunan Province for Innovation Group, China (No. 09JJ7004), and the Key Special Program for Science and Technology of Hunan Province, China (No. 2009FJ1002).

REFERENCES

- [1] Y.Q. Guo, Y.M. Li, F. Bogard, K. Debray, J. Mater. Process. Technol. 151 (2004) 88–97.
- [2] V. Pegada, Y. Chun, S. Santhanam, J. Mater. Process. Technol. 125 (2002) 743–750.
- [3] M. Gavas, M. Izciler, Mater. Des. 28 (2007) 1641–1646.
- [4] Z.Q. Sheng, S. Jirathearanat, T. Altan, Int. J. Mach. Tools Manuf. 44 (2004) 487–494.
- [5] J. Cao, M.C. Boyce, J. Eng. Mater. Technol. 119 (1997) 354–365.
- [6] S.P. Keeler, Sheet Metal Industries 42 (1965) 683–691.
- [7] Z. Marciniak, K. Cuczynski, Int. J. Mech. Sci. 9 (1967) 613–620.
- [8] T.B. Stoughton, Int. J. Mech. Sci. 42 (2000) 1–27.
- [9] J.W. Signorelli, M.A. Bertinetti, P.A. Turner, Int. J. Plasticity 25 (2009) 1–25.
- [10] X. Hu, Z.Q. Lin, S.H. Li, Y.X. Zhao, Mater. Des. 31 (2010) 1410–1416.
- [11] Y.Q. Guo, J.L. Batoz, J.M. Detraux, Int. J. Numer. Meth. Eng. 30 (1990) 1385–1401.
- [12] M. Khelifa, M. Oudjene, J. Mater. Process. Technol. 200 (2008) 71–76.
- [13] K. Saanouni, Eng. Fract. Mech. 75 (2008) 3545–3559.
- [14] J.P. Fan, C.Y. Tang, C.P. Tsui, L.C. Chan, T.C. Lee, Int. J. Mach. Tools Manuf. 46 (2006) 1035–1044.
- [15] M. Zhou, Y. Zhang, L. Cai, J. Appl. Phys. 91 (2002) 5501–5503.
- [16] A.G. Mamalis, D.E. Manolakos, A.K. Baldoukas, J. Mater. Process. Technol. 68 (1997)

71–75.

- [17] L.Q. Zhou, J.G. Tang, Y.P. Li, Y.C. Zhou, *J. Mater. Process. Technol.* 206 (2008) 431–437.
- [18] Z.S. Ma, Y.C. Zhou, S.G. Long, C.S. Lu, *J. Mater. Sci. Technol.* 28 (2012) 626–635.
- [19] V. Burokas, A. Martusiene, G. Bikulcius, *Surf. Coat. Technol.* 102 (1998) 233–236.
- [20] S. Kapinski, *J. Mater. Process. Technol.* 60 (1996) 197–200.
- [21] H. Takuda, K. Mori, H. Fujimoto, N. Hatta, *J. Mater. Process. Technol.* 60 (1996) 291–296.
- [22] L.H. Xiao, X.P. Su, J.H. Wang, Y.C. Zhou, *Mater. Sci. Eng. A* 501 (2009) 235–241.
- [23] M.R. Morovvati, B. Mollaei-Dariani, M.H. Asadian-Ardakani, *J. Mater. Process. Technol.* 210 (2010) 1738–1747.
- [24] H. Hooputra, H. Gese, H. Dell, H. Werner, *Int. J. Crashworthiness* 9 (2004) 449–464.
- [25] T.J. Wang, *Eng. Fract. Mech.* 51 (1995) 275–279.
- [26] Y. Li, M. Luo, J. Gelarch, T. Wierzbicki, *J. Mater. Process. Technol.* 210 (2010) 1858–1869.
- [27] M. Ahmetoglu, T.R. Broek, G. Kinzel, T. Altan, *CIRP Ann-Manuf. Technol.* 44 (1995) 247–250.
- [28] Y.G. Liao, Y.C. Zhou, Y.L. Huang, L.M. Jiang, *Mech. Mater.* 41 (2009) 308–318.
- [29] L.P. Moreira, G. Ferron, G. Ferran, *J. Mater. Process. Technol.* 108 (2000) 78–86.
- [30] C. Arwidson, *Numerical Simulation of Sheet Metal Forming for High Strength Steels*, Ph.D. Thesis, Lulea University of Technology, 2005.
- [31] L.Q. Zhou, Y.P. Li, Y.C. Zhou, *J. Mater. Eng. Perform.* 15 (2006) 287–294.

Figures and table captions

Table 1 Mechanical properties of MSNC, where substrate and coating are low carbon steel sheet and nickel coating

Fig. 1 Schematic diagram of the failure modes: (a) wrinkling and (b) fracture.

Fig. 2 Schematic diagram of the model: (a) configures of the tool and coated metal sheet and (b) their geometric dimensions.

Fig. 3 Finite element model and meshes used in simulations: (a) a quarter model, (b) finite element meshes of a whole blank, and (c) meshes in plane and thickness directions.

Fig. 4 Simulations at punch displacements of 4 mm, 6 mm, 8 mm and 10 mm in the case of wrinkling: (a) the damage distribution along a path from center to edge in nickel coating, (b) the damage distribution, (c) the stress distribution in the thickness direction, σ_{22} and (d) the true strain distribution in the thickness direction, ε_{22} .

Fig. 5 Simulations at punch displacements of 4 mm, 6 mm, 8 mm and 10 mm in the case of success: (a) the damage distribution along a path from center to edge in nickel coating, (b) the damage contour, (c) the stress distribution in the thickness direction, σ_{22} and (d) the true strain distribution in the thickness direction, ε_{22} .

Fig. 6 Simulations at punch displacements of 4 mm, 6 mm, 8 mm and 10 mm in the case of fracture: (a) the damage distribution along a path from center to edge in nickel coating, (b) the damage distribution, (c) the stress distribution in the thickness direction, σ_{22} and (d) the true strain distribution in the thickness direction, ε_{22} .

Fig. 7 Relationship between the punch displacement and damage in the cases of wrinkling, success and fracture: (a) in the flange area and (b) at the punch radius.

Fig. 8 Relationship between the punch displacement and maximum principal strain in the flange area in the cases of wrinkling, success and fracture.

Fig. 9 Relationship between the punch displacement and maximum principal strain at the punch radius in the cases of (a) fracture and (b) wrinkling and success.

Fig. 10 Deformation shapes with different punch displacements of blank in simulations: (a) fracture with BHF = 2 kN, (b) success with BHF = 1.5 kN, and (c) wrinkling with BHF = 1 kN.

Fig. 11 Punch load-displacement curves of simulation and experiment in the case of fracture.

Fig. 12 Punch load-displacement curves of simulation and experiment in the case of wrinkling.

Fig. 13 Punch load-displacement curves of simulation and experiment in the case of success.

Fig. 14 Forming limit diagram of three cases in simulations: fracture, success and wrinkling.

Table list

Table 1

	E (GPa)	σ_y (μm)	ν	n
Substrate	209.9	264.4	0.27	0.12
Coating	215.0	470.0	0.30	0.13

Figure List

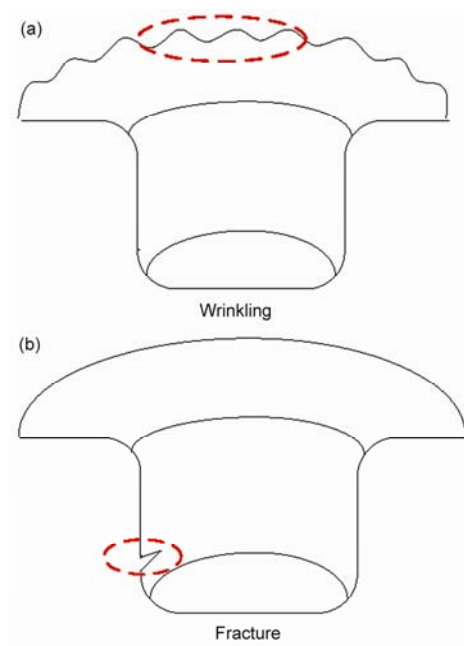


Fig. 1

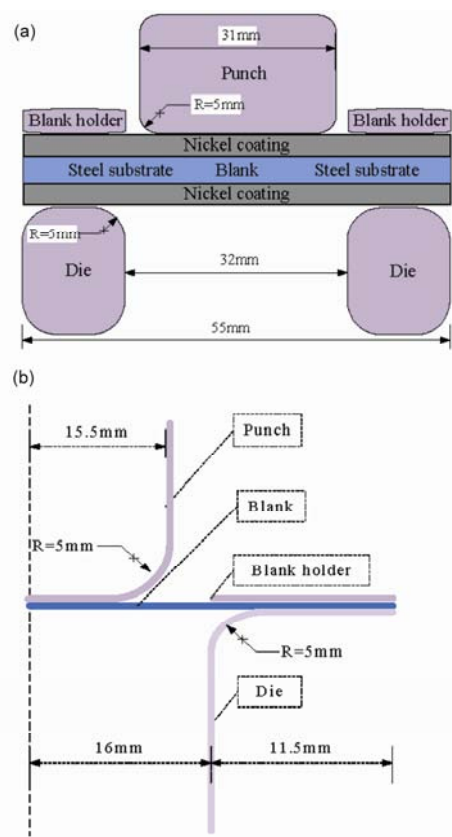


Fig. 2

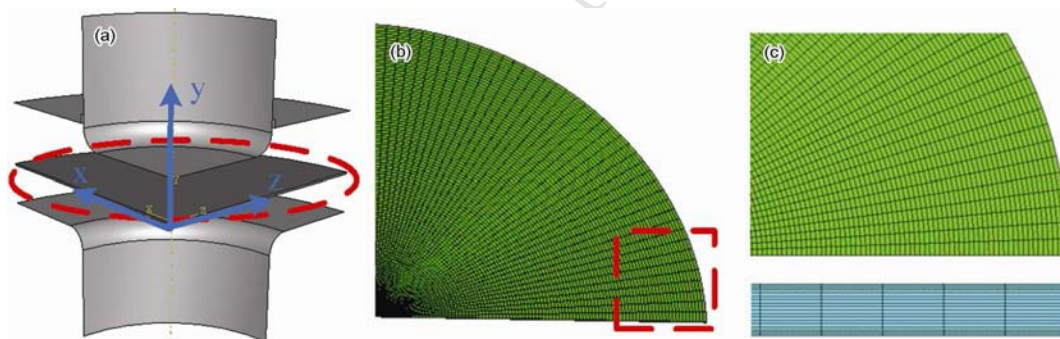


Fig. 3

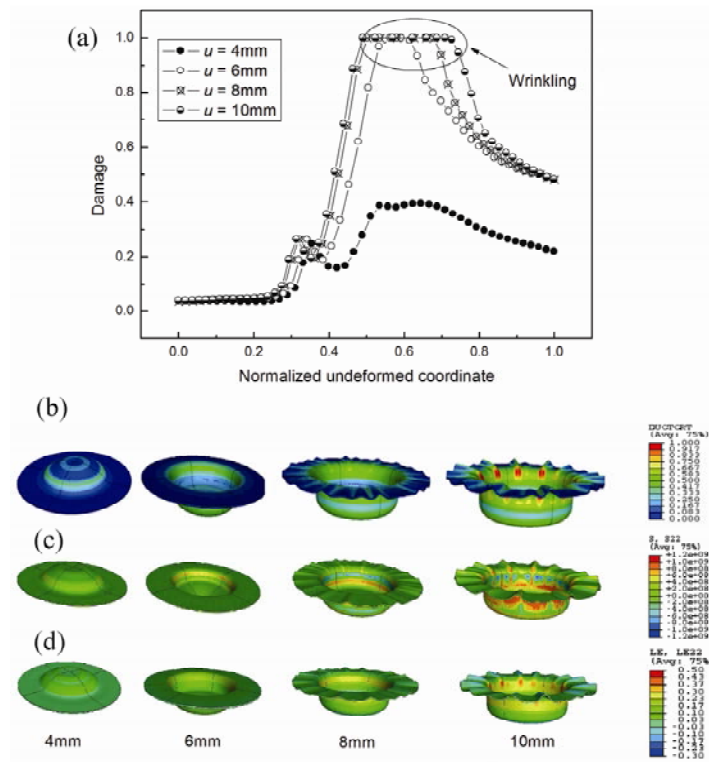


Fig. 4

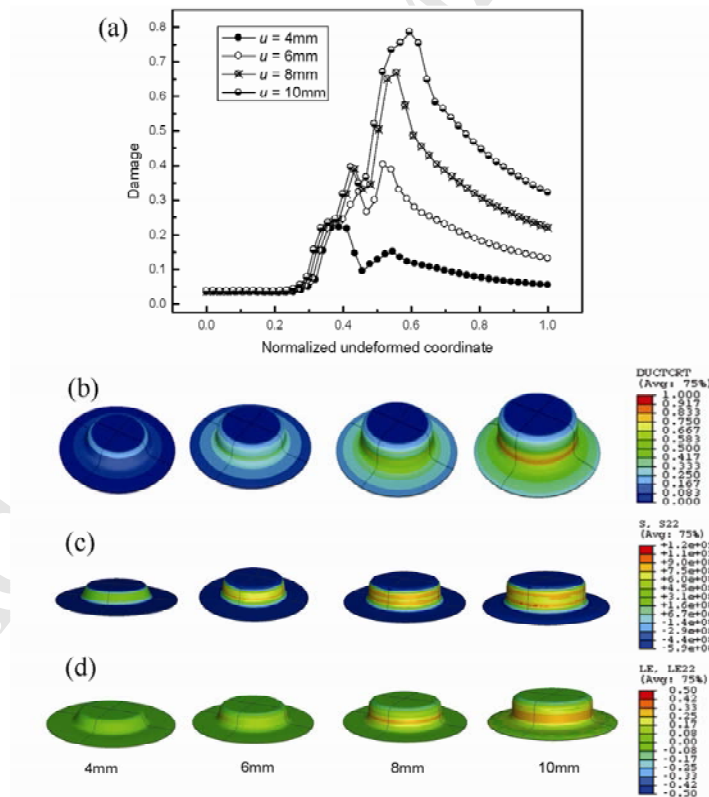


Fig. 5

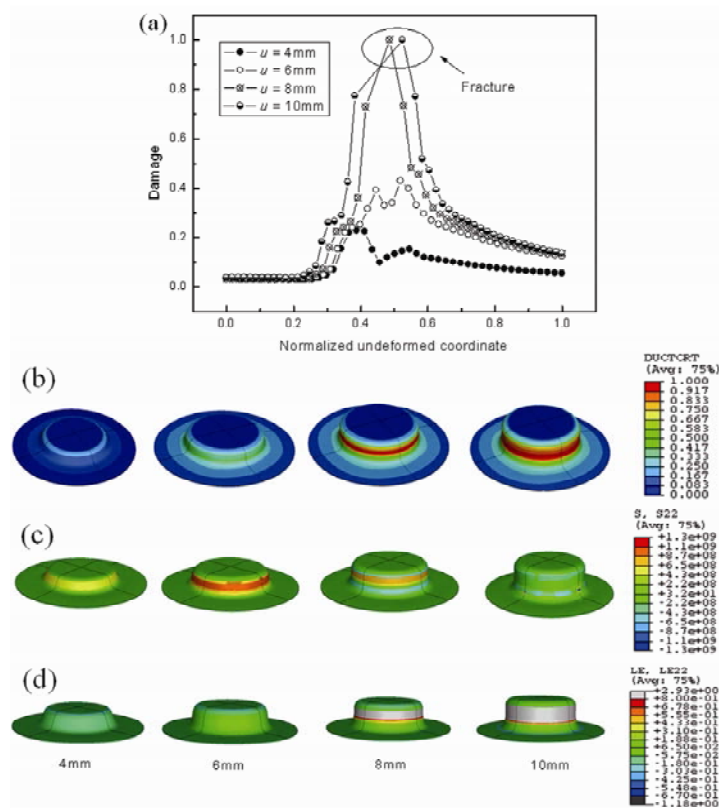


Fig. 6

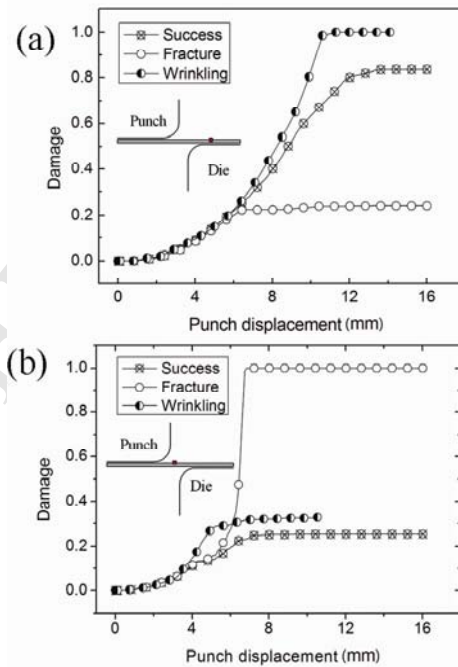


Fig. 7

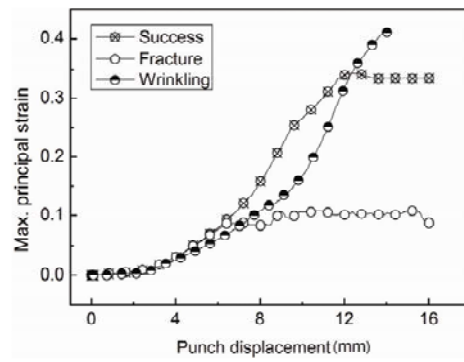


Fig. 8

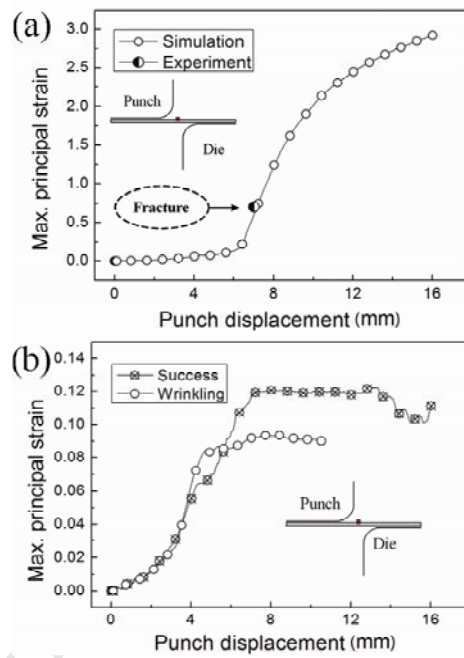


Fig. 9

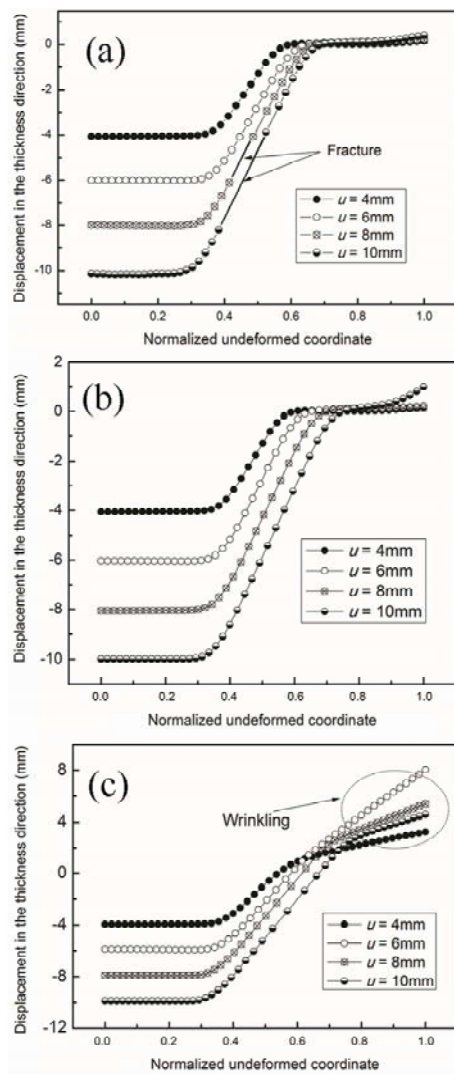


Fig. 10

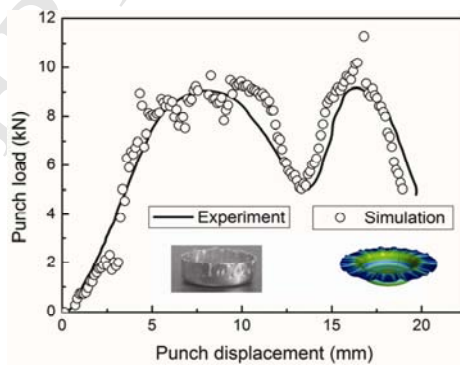


Fig. 11

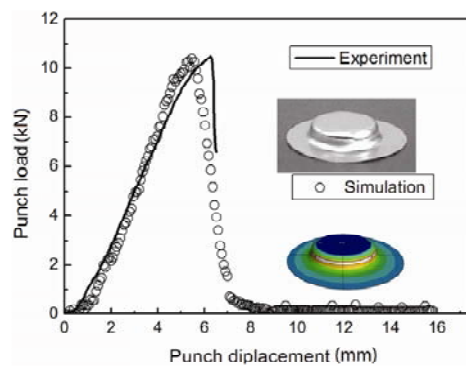


Fig. 12

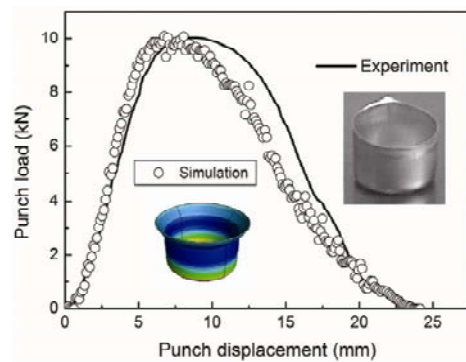


Fig. 13

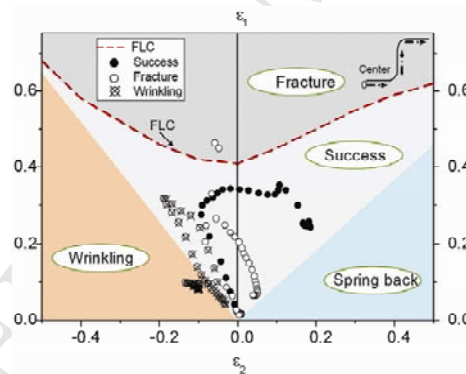


Fig. 14